



Supported by



Accepted Article

Title: Selective C-O Bond Cleavage of Bio-Based Organic Acids over Palladium Promoted MoOx/TiO₂

Authors: Yomaira J. Pagan-Torres, Ayad Nancy, Lucas Freitas de Lima e Freitas, Sandra Albarracín-Suazo, Génesis Ruiz-Valentín, Charles A. Roberts, and Eranda Nikolla

This manuscript has been accepted after peer review and appears as an Accepted Article online prior to editing, proofing, and formal publication of the final Version of Record (VoR). This work is currently citable by using the Digital Object Identifier (DOI) given below. The VoR will be published online in Early View as soon as possible and may be different to this Accepted Article as a result of editing. Readers should obtain the VoR from the journal website shown below when it is published to ensure accuracy of information. The authors are responsible for the content of this Accepted Article.

To be cited as: *ChemCatChem* 10.1002/cctc.202001799

Link to VoR: <https://doi.org/10.1002/cctc.202001799>

COMMUNICATION

Selective C-O Bond Cleavage of Bio-Based Organic Acids over Palladium Promoted MoO_x/TiO₂

Ayad Nancy,^{[+][a]} Lucas Freitas de Lima e Freitas,^{[+][b]} Sandra Albarracín-Suazo,^[a] Génesis Ruiz-Valentín,^[a] Charles A. Roberts,^[c] Eranda Nikolla^{*[b]} and Yomaira J. Pagán-Torres^{*[a]}

[a] Dr. A. Nancy, S. Albarracín-Suazo, G. Ruiz-Valentín, Prof. Dr. Y. J. Pagán-Torres

Department of Chemical Engineering
University of Puerto Rico-Mayagüez Campus
Mayagüez, PR 00680 (USA)
E-mail: yomairaj.pagan@upr.edu

[b] L. F. de L. e Freitas, Prof. Dr. E. Nikolla
Department of Chemical Engineering and Materials Science

Wayne State University
Detroit, MI 48202 (USA)

E-mail: erandan@wayne.edu

[c] Dr. C. A. Roberts
Toyota Research Institute – North America
Ann Arbor, MI 48105 (USA)

[+] The authors A. Nancy and L. F. de L. e Freitas contributed equally to this article.

Supporting information for this article is given via a link at the end of the document.

Abstract: Hydrodeoxygenation chemistries play a key role in the upgrading of biomass-derived feedstocks. Among these, the removal of targeted hydroxyl groups through selective C-O bond cleavage from molecules containing multiple functionalities over heterogeneous catalysts has shown to be a challenge. Herein, we report a highly selective and stable heterogeneous catalyst for hydrodeoxygenation of tartaric acid to succinic acid. The catalyst consists of reduced Mo⁵⁺ centers promoted by palladium, which facilitate selective C-O bond cleavage, while leaving intact carboxylic acid end groups. Stable catalytic performance over multiple cycles is demonstrated. This catalytic system opens up opportunities for selective processing of biomass derived sugar acids with a high degree of chemical functionality.

Currently, fossil fuels represent the primary source of energy, fuel, and commodity chemical production.^[1] However, escalating concerns about the environmental effect of their utilization and their inevitable depletion have urged the discovery and development of environmentally benign processes.^[2] Succinic acid (SA) is a highly desired drop-in bio-based building block, with an estimated market value of USD 130 million/year (in 2018).^[3] SA is mainly produced via thermocatalytic processing of petroleum-based n-butane.^[3b, c] This process involves complex purification steps and is highly dependent on the crude-oil cost.^[3c] Recently, bio-based SA was manufactured via fermentation of glucose using engineered micro-organisms.^[3c, 4] This route suffered from significant drawbacks, including low productivity, high nutrient requirements, the formation of organic acid byproducts, along with a costly downstream recovery and purification of the final product.^[3c, 4-5] Synthesis of SA from tartaric acid (TA) was reported via a two-step process that involved the deoxydehydration (DODH) of TA to maleic acid (ME) in 3-pentanol (both as reductant and solvent) with NH₄ReO₄, followed by hydrogenation of ME to SA over Pt/C in water. While the system yielded 86% SA, it required the utilization of two precious metal catalysts and multiple processing steps.^[6] To overcome

some of these challenges, a thermocatalytic one-step process to produce SA from TA over a MoO_x/carbon black (BC) catalyst was developed.^[7] Characterization studies revealed the presence of a partially reduced MoO_x/BC surface that promoted C-O bond cleavage. Despite the high SA yield (87%) reported, the need for catalyst pretreatment and reaction initiators (HBr and acetic acid) to activate the C-O bond cleavage added complexity to the process. Production of dimethyl succinate via deoxydehydration (DODH) of tartaric acid or diethyl tartrate was also demonstrated over a multicomponent, complex catalytic system comprised of a homogeneous KReO₄, Pd/C, H₃PO₄, and activated carbon yielding 88% of methyl succinate under hydrogen atmosphere.^[8] In this case, the complex reaction pool presented significant challenges for product separation.

Herein, we report on a highly active, selective and stable heterogeneous catalytic system comprising of supported reducible metal oxide species coupled with a hydrogenating metal for selective HDO of TA to form SA with 92% yield (SA selectivity of 93% and TA conversion of 99%) upon 16 hours of reaction. We show that the dominant catalytic pathway involves sequential HDO of TA to malic acid (MA) and MA to SA. In this catalytic cycle, C-O bond cleavage was catalyzed by reduced Mo⁵⁺ sites formed in-situ in the presence of Pd and hydrogen. The catalyst showed stability upon multiple reuse cycles.

Table 1 summarizes the TA HDO performance of various catalysts containing hydrogenating noble metals (e.g., Pd (Entry 1), Rh (Entry 2), and Pt (Entry 3)) coupled with MoO_x supported on TiO₂. The Pd-containing catalyst resulted in 80% SA selectivity at a TA conversion of 65% and the highest SA formation rate of 13.6 x 10⁻⁷ mole g_{cat}⁻¹ s⁻¹. High amounts of fumaric acid (FA) were detected in the case of the Pt-containing catalyst (Entry 3, Table 1) potentially suggesting strong adsorption of carboxylic acid groups on the Pt surface, blocking hydrogenation sites. The effect of the nature of the dispersed metal oxide species (MoO_x, WO_x, ReO_x, VO_x) in the presence of Pd (the best performing hydrogenating metal) on the catalytic performance is shown in Entries 1, 4, 5, and 6 of Table 1, respectively. We find that the

COMMUNICATION

Table 1. Catalytic performance of supported catalysts in the hydrodeoxygenation of tartaric acid.^[a]

| Entry | Catalyst | Conv. (%) | Product Selectivity (%) | | | | SA formation rate (x 10 ⁻⁷ mole g _{cat} ⁻¹ s ⁻¹) ^[b] |
|-------|---|-----------|-------------------------|----|----|----|--|
| | | | | | | | |
| 1 | 4 wt % MoO _x -0.3 wt % Pd/TiO ₂ | 65 | 18 | <1 | 0 | 80 | 13.6 |
| 2 | 4 wt % MoO _x -0.3 wt % Rh/TiO ₂ | 62 | 18 | 0 | 0 | 78 | 12.2 |
| 3 | 4 wt % MoO _x -0.3 wt % Pt/TiO ₂ | 62 | 17 | 24 | 0 | 51 | 7.6 |
| 4 | 4 wt % WO _x -0.3 wt % Pd/TiO ₂ | 22 | 20 | 0 | 0 | 50 | 2.0 |
| 5 | 4 wt % ReO _x -0.3 wt % Pd/TiO ₂ | 12 | 9 | 0 | 0 | 64 | 1.4 |
| 6 | 4 wt % VO _x -0.3 wt % Pd/TiO ₂ | <2 | 2 | 0 | 0 | 6 | ~0 |
| 7 | 4 wt % MoO _x -0.3 wt % Pd/ZrO ₂ | 8 | 32 | 0 | 0 | 55 | 0.8 |
| 8 | 4 wt % MoO _x -0.3 wt % Pd/SiO ₂ | 6 | 20 | 0 | 0 | 28 | 0.3 |
| 9 | 0.3 wt % Pd/TiO ₂ | 8 | 29 | 0 | 0 | 15 | 0.2 |
| 10 | 4 wt % MoO _x /TiO ₂ | 11 | 7 | 12 | 18 | 3 | 0.1 |
| 11 | TiO ₂ | 7 | 7 | 2 | 15 | 0 | — |

[a] Reaction conditions: 2 wt % TA in 1,4-dioxane, 433 K, 500 psi H₂, t = 2 h, W_{cat} = 0.26 g. [b] SA formation rates are reported for TA conversions <25%.

MoO_x containing catalyst (Entry 1) resulted in >6 times higher SA formation rates than the other metal oxide systems. In the case of support effects (TiO₂, ZrO₂, and SiO₂), TiO₂ (Entry 1, Table 1) led to the highest TA conversion and SA selectivity compared to ZrO₂ (Entry 7) and SiO₂ (Entry 8). The observed support-dependent catalytic performance could be associated to variations in the dispersion and reducibility of molybdenum oxide species on TiO₂, ZrO₂, and SiO₂ supports.^[9] Furthermore, it has been shown that hydrogen spillover occurs at higher rates over noble metals supported on reducible oxides (i.e., TiO₂) compared to nonreducible oxides (i.e., ZrO₂) which potentially could be another reason for the observed support-dependent catalytic performance.^[10] Overall, Table 1 shows that MoO_x coupled with Pd supported on TiO₂ (4 wt % MoO_x-0.3 wt % Pd/TiO₂) exhibited the highest conversion and selectivity for TA HDO among all catalysts considered containing both supported noble metal and dispersed metal oxide species. For monometallic supported catalysts (Pd/TiO₂ and MoO_x/TiO₂) (Table 1, Entry 9 and 10) and the TiO₂ support (Entry 11), SA formation rates lower than 0.2 x 10⁻⁷ mole g_{cat}⁻¹ s⁻¹ were observed. CO chemisorption measurements (Table S1) show that the CO uptake on the catalyst containing both Pd and MoO_x supported on TiO₂ (25.5 ± 0.8 μmol g⁻¹) was higher than the individual and combined CO uptakes on Pd/TiO₂ (4.4 ± 0.8 μmol g⁻¹) and MoO_x/TiO₂ (11.3 ± 3.3 μmol g⁻¹) at the same weight loadings. The increase in CO uptake for 4 wt % MoO_x-0.3 wt % Pd/TiO₂ is likely due to an enhanced dispersion of MoO_x species in the combined catalytic system. Thus, all three components (MoO_x, Pd, and TiO₂) are deemed necessary to achieve dispersed catalytic sites leading to high SA production rates from TA HDO.

Mo and Pd loading effects on TiO₂ were studied for TA HDO (Figures S1-2). In the case of Mo loading (Figure S1), the highest SA formation rate was obtained for 4 wt % of Mo. As we discuss below, this is a consequence of the MoO_x species formed on the surface as a function of loading (Figure S1). Conversely, no

significant changes in the TA conversions and SA selectivities were observed above 0.3 wt % Pd loading (Figure S2). These results suggest that Pd acts mainly as a promoter for molecular hydrogen dissociation at weight loadings equal or higher than 0.3 wt %.

To gain insights on the reaction pathway, time-course studies of TA HDO on 4 wt % MoO_x-0.3 wt % Pd supported on TiO₂ were performed (Figure S3). Two primary reaction intermediates were observed: (i) MA as the main intermediate, and (ii) FA, which forms at an early stage of the reaction followed by complete disappearance after 90 min. This suggests that the main reaction pathway involves the direct C-O bond cleavage of TA to MA followed by a sequential C-O bond cleavage to SA. To extract apparent activation energies, SA formation rates as a function of temperature were obtained (Figure S4 and Table S2) under differential conditions. We find that the apparent activation energy for this process is 79 ± 4.9 kJ/mol consistent with reported HDO apparent barriers.^[11]

Characterization of the MoO_x-Pd/TiO₂ systems was performed to elucidate the nature of the catalytic sites. XRD patterns show peaks at 23° and 34° (correlate to (110) and (111) planes, respectively) consistent with crystalline MoO₃ for 6 wt % MoO_x-0.3 wt % Pd/TiO₂ and 10 wt % MoO_x-0.3 wt % Pd/TiO₂, while no peaks related to crystalline MoO₃ were observed for 4 wt % MoO_x-0.3 wt % Pd/TiO₂ catalyst (Figure 1a), pointing to the potential dispersed polymeric nature of MoO_x species. The XRD patterns of the fresh and spent catalysts show no significant structural changes of the catalysts after reaction, suggesting that these phases are preserved under reaction conditions (Figure S5). Figure 1b shows the Raman spectra of 6 wt % MoO_x-0.3 wt % Pd/TiO₂ and 10 wt % MoO_x-0.3 wt % Pd/TiO₂ characterized by peaks at 821 and 997 cm⁻¹, corresponding to the stretching vibrations of Mo-O-Mo and Mo=O in crystalline MoO₃, respectively, consistent with observations from XRD.^[12] Whereas, for 4 wt % MoO_x-0.3 wt % Pd/TiO₂, a Raman band at 981 cm⁻¹

COMMUNICATION

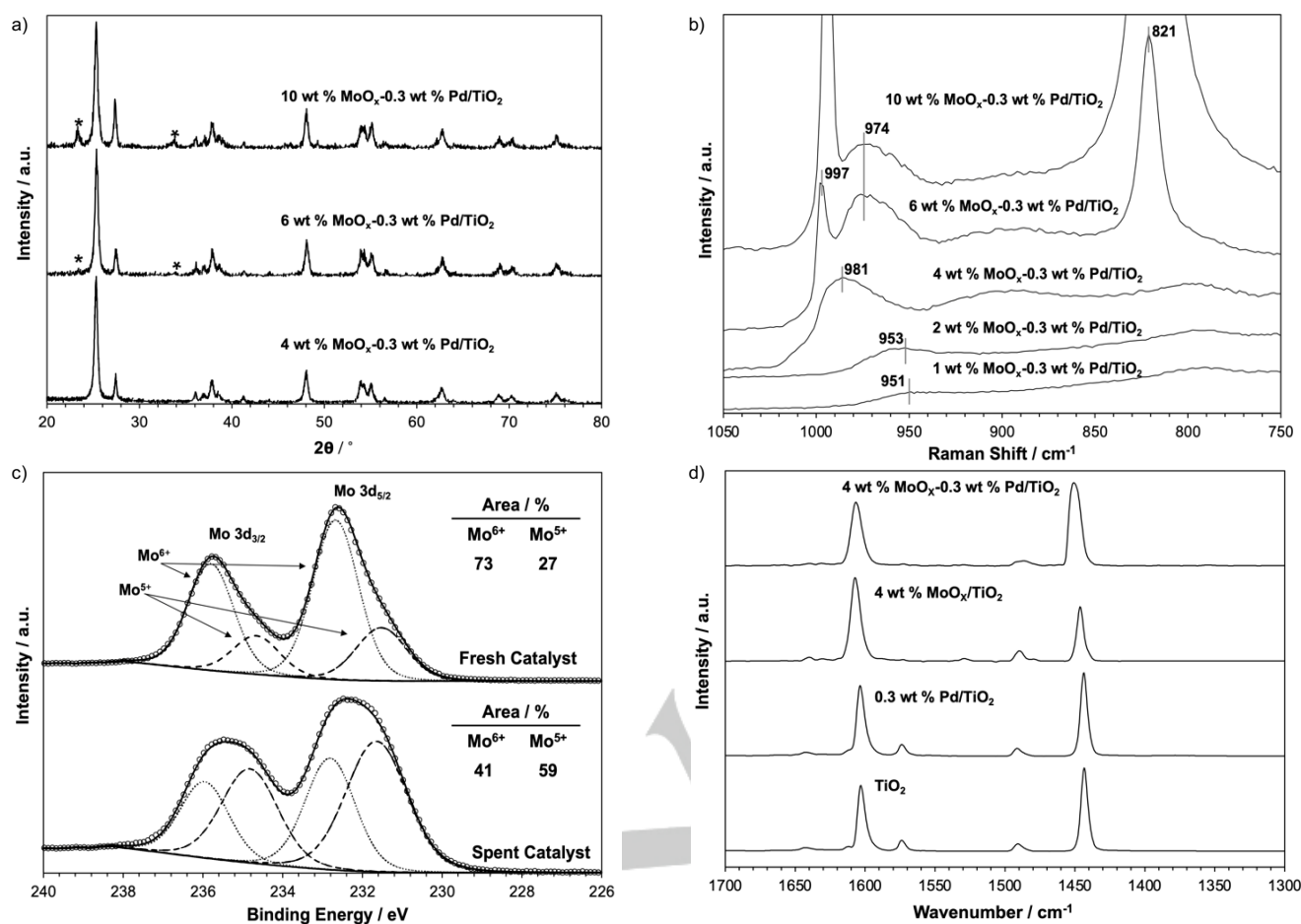


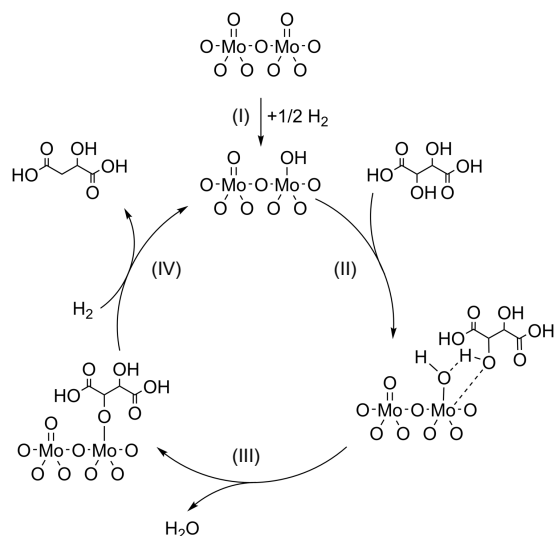
Figure 1. (a) X-ray diffraction patterns of 4 wt % MoO_x-0.3 wt % Pd/TiO₂, 6 wt % MoO_x-0.3 wt % Pd/TiO₂ and 10 wt % MoO_x-0.3 wt % Pd/TiO₂. The (*) indicates the crystalline phase of MoO₃. (b) Raman Spectra of 1 wt % MoO_x-0.3 wt % Pd/TiO₂, 2 wt % MoO_x-0.3 wt % Pd/TiO₂, 4 wt % MoO_x-0.3 wt % Pd/TiO₂, 6 wt % MoO_x-0.3 wt % Pd/TiO₂, 10 wt % MoO_x-0.3 wt % Pd/TiO₂. (c) XPS spectra of the (3d) Mo energy region for fresh and spent 4 wt % MoO_x-0.3 wt % Pd/TiO₂ after TA HDO. (d) FTIR spectra of adsorbed pyridine on 4 wt % MoO_x-0.3 wt % Pd/TiO₂ after catalyst reduction at 433 K for 1 h.

was observed, attributable to the symmetric stretching mode of the terminal Mo=O in surface polymeric octahedral molybdena species.^[12] For catalytic systems with Mo loadings of less than 4 wt %, a Raman band at ~951 cm⁻¹ was observed, which was assigned to the stretching vibration of Mo=O in tetrahedral Mo oxide species.^[12] To further shed light on the oxidation state of molybdenum on the surface of 4 wt % MoO_x-0.3 wt % Pd/TiO₂, the catalyst before and after reaction was studied by X-ray photoelectron spectroscopy (XPS) (Figure 1c). The fresh catalyst featured mainly a Mo⁶⁺ oxidation state, while the spent catalyst exhibited a 3/2 ratio of Mo⁵⁺/Mo⁶⁺ states.^[13] This suggests that reduction of molybdenum oxide occurred under reaction conditions in the presence of hydrogen and Pd. These results coupled with Raman studies provide strong evidence that the surface of the highest performing 4 wt % MoO_x-0.3 wt % Pd/TiO₂ catalyst is uniquely dominated by octahedral Mo oxide species containing oxygen vacancies, which act as active sites. Diffuse Reflectance Infrared Fourier Transform Spectroscopy (DRIFTS) studies with adsorbed pyridine on reduced 4 wt % MoO_x-0.3 wt % Pd/TiO₂ show dominant bands at ~1442 cm⁻¹, 1486 cm⁻¹, 1570 cm⁻¹, 1606 cm⁻¹ corresponding to Lewis acid sites (Figure 1d), with no significant contribution from bands (1540 cm⁻¹ and 1638 cm⁻¹) associated with Bronsted acidity.^[14] These results are consistent with the metal cationic centers in 4 wt % MoO_x-0.3 wt % Pd/TiO₂ acting as Lewis acid sites.^[14a, 15]

Based on the insights from the kinetic and characterization studies, the proposed catalytic cycle for HDO of TA to SA over 4 wt % MoO_x-0.3 wt % Pd/TiO₂ is shown in Scheme 1. We suggest that the main role of Pd is to activate molecular hydrogen, which assists in the reduction of high valent Mo⁶⁺ to Mo⁵⁺ species (I). This is consistent with XPS pointing to a dominant Mo⁵⁺ oxidation state for the spent catalyst. This results in the formation of reduced Mo⁵⁺ centers, which coordinate with the internal hydroxyl groups of TA (II), leading to proton removal through water formation (III). This is followed by C-O bond cleavage and MA formation (IV) leaving behind a hydroxylated Mo site, consistent with the time-study in Figure S3 showing the formation of MA as the main intermediate. The hydroxylated Mo site is reduced in the presence of hydrogen (IV), regenerating surface Mo⁵⁺ to assist with the subsequent C-O bond cleavage of MA to SA. This catalytic cycle is consistent with direct HDO mechanisms on redox metal centers.^[16]

Catalytic stability studies of 4 wt % MoO_x-0.3 wt % Pd/TiO₂ for TA HDO are shown in Figure 2. No significant losses in conversion and selectivity were observed as a function of cycling demonstrating the stability of the catalyst. This was also confirmed via post characterization using XRD (Figure S5), ICP and CO chemisorption studies (Table S1), which showed no significant changes in the catalyst structure as a function of cycling.

COMMUNICATION



Scheme 1. Proposed reaction mechanism for MoO_x-Pd/TiO₂ catalyzed HDO of TA to MA.

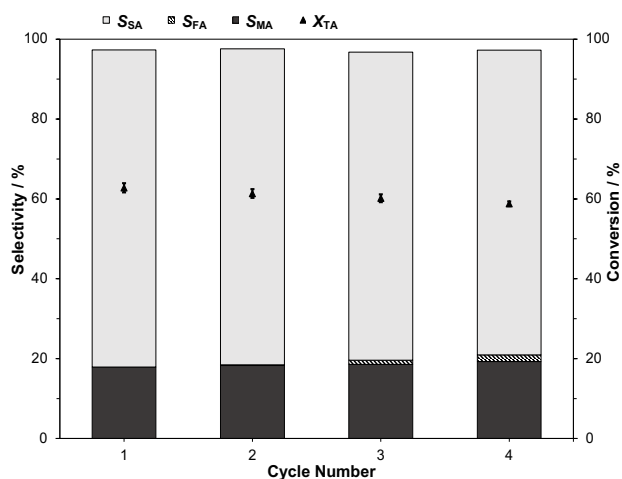


Figure 2. Catalyst cyclability studies (conversion (X_{TA}) and selectivity (S)) for TA HDO over 4 wt % MoO_x-0.3 wt % Pd/TiO₂. Reaction Conditions: 2 wt % TA in 1,4-dioxane, T = 433 K, P_{H₂} = 500 psi, t = 2 h, W_{cat} = 0.26 g.

In conclusion, we have demonstrated that 4 wt % MoO_x-0.3 wt % Pd/TiO₂ is an active, selective and stable catalyst for HDO of TA to SA. This catalyst exhibits SA turnover rates of 13.6×10^{-7} mole g_{cat}⁻¹ s⁻¹, the highest among the reported heterogeneous catalysts. We show that the redox properties of MoO_x are superior to those of ReO_x, VO_x, WO_x under similar reaction conditions making it the optimal catalytic center for C-O bond cleavage through an oxygen vacancy driven reaction mechanism.

Acknowledgements

A.N., G.R.V and Y.J.P.T gratefully acknowledge financial support for this research from the National Science Foundation through CBET Award No. 1817297. S.A.S acknowledges financial support from the National Science Foundation Award No. OIA-1632824. L.F.L.F. and E.N. gratefully acknowledge financial support from the National Science Foundation for funding this research through DMREF Grant No. 1436206. The authors thank Gerardo Rivera-Castro and Tania Class-Martínez for assistance

in catalyst synthesis and kinetic studies. The authors also thank the Lumigen Instrument Center at Wayne State University for the use of the X-ray diffraction/spectroscopy (National Science Foundation MRI-1427926, MRI-1849578).

Keywords: succinic acid • sustainable chemistry • hydrodeoxygenation • heterogeneous catalysis • C-O bond cleavage

[1] a) D. M. Alonso, S. H. Hakim, S. Zhou, W. Won, O. Hosseinaei, J. Tao, V. Garcia-Negron, A. H. Motagamwala, M. A. Mellmer, K. Huang, C. J. Houtman, N. Labbé, D. P. Harper, C. T. Maravelias, T. Runge, J. A. Dumesic, *Sci. Adv.* **2017**, *3*, 1-7; b) A. Corma, S. Iborra, A. Velty, *Chem. Rev.* **2007**, *107*, 2411-2502.

[2] a) M. Balakrishnan, E. R. Sacia, S. Sreekumar, G. Gunbas, A. A. Gokhale, C. D. Scown, F. D. Toste, A. T. Bell, *Proc. Natl. Acad. Sci. U. S. A.* **2015**, *112*, 7645-7649; b) M. Wang, J. Ma, H. Liu, N. Luo, Z. Zhao, F. Wang, *ACS Catal.* **2018**, *8*, 2129-2165; c) S. Li, W. Deng, S. Wang, P. Wang, D. An, Y. Li, Q. Zhang, Y. Wang, *ChemSusChem* **2018**, *11*, 1995-2028; d) T. W. Walker, A. H. Motagamwala, J. A. Dumesic, G. W. Huber, *J. Catal.* **2019**, *369*, 518-525.

[3] a) T. Werpy, G. Petersen, *Top Value Added Chemicals from Biomass Volume I - Results of Screening for Potential Candidates from Sugars and Synthesis Gas*, Pacific Northwest National Laboratory and National Renewable Energy Laboratory, **2004**; b) A. Carlson, B. Coggio, K. Lau, C. Mercogliano, J. Millis, in *Chemicals and Fuels from Bio - Based Building Blocks, Vol. 1* (Eds.: F. Cavani, S. Albonetti, F. Basile, A. Gandini), Wiley-VCH, **2016**, pp. 173-190; c) S. Vaswani, SRI Consulting, Menlo Park, CA, **2010**, pp. 42-42.

[4] J. Akhtar, A. Idris, R. Abd. Aziz, *Appl. Microbiol. Biotechnol.* **2014**, *98*, 987-1000.

[5] K.-K. Cheng, X.-B. Zhao, J. Zeng, R.-C. Wu, Y.-Z. Xu, D.-H. Liu, J.-A. Zhang, *Appl. Microbiol. Biotechnol.* **2012**, *95*, 841-850.

[6] X. Li, Y. Zhang, *ChemSusChem* **2016**, *9*, 2774-2778.

[7] J. Fu, E. S. Vasiliadou, K. A. Goulas, B. Saha, D. G. Vlachos, *Catal. Sci. Technol.* **2017**, *7*, 4944-4954.

[8] R. T. Larson, A. Samant, J. Chen, W. Lee, M. A. Bohn, D. M. Ohmann, S. J. Zuend, F. D. Toste, *J. Am. Chem. Soc.* **2017**, *139*, 14001-14004.

[9] C. V. Cáceres, J. L. G. Fierro, J. Lázaro, A. López Agudo, J. Soria, *J. Catal.* **1990**, *122*, 113-125.

[10] W. Karim, C. Spreafico, A. Kleibert, J. Gobrecht, J. VandeVondele, Y. Ekinci, J. A. van Bokhoven, *Nature* **2017**, *541*, 68-71.

[11] Y. Xi, J. Lauterbach, Y. Pagan-Torres, A. Heyden, *Catal. Sci. Technol.* **2020**, *10*, 3731-3738.

[12] a) H. Hu, I. E. Wachs, S. R. Bare, *J. Phys. Chem.* **1995**, *99*, 10897-10910; b) G. Tsilomelekis, S. Boghosian, *Catal. Sci. Technol.* **2013**, *3*, 1869-1888.

[13] K. Murugappan, E. M. Anderson, D. Teschner, T. E. Jones, K. Skorupska, Y. Román-Leshkov, *Nat. Catal.* **2018**, *1*, 960-967.

[14] a) W. Suarez, J. A. Dumesic, C. G. Hill, *J. Catal.* **1985**, *94*, 408-421; b) D. D. Falcone, J. H. Hack, A. Y. Klyushin, A. Knop-Gericke, R. Schlögl, R. J. Davis, *ACS Catal.* **2015**, *5*, 5679-5695.

[15] J. D. Kammert, J. Xie, I. J. Godfrey, R. R. Unocic, E. Stavitski, K. Attenkofer, G. Sankar, R. J. Davis, *ACS Sustainable Chem. Eng.* **2018**, *6*, 12353-12366.

[16] a) Y. Amada, H. Watanabe, M. Tamura, Y. Nakagawa, K. Okumura, K. Tomishige, *J. Phys. Chem. C* **2012**, *116*, 23503-23514;

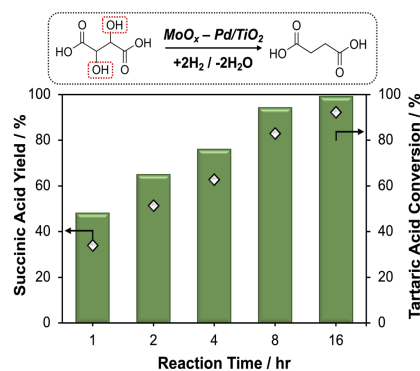
b) N. Ota, M. Tamura, Y. Nakagawa, K. Okumura, K. Tomishige, *Angew. Chem. Int. Ed.* **2015**, *54*, 1897-1900; c) N. Ota, M. Tamura, Y. Nakagawa, K. Okumura, K. Tomishige, *ACS Catal.* **2016**, *6*, 3213-3226; d) K. Tomishige, Y. Nakagawa, M. Tamura, *Green Chem.* **2017**,

19, 2876-2924; e) M. Shetty, E. M. Anderson, W. H. Green, Y. Román-Leshkov, *J. Catal.* **2019**, *376*, 248-257; f) L. Sandbrink, K. Beckerle, I. Meiners, R. Liffmann, K. Rahimi, J. Okuda, R. Palkovits, *ChemSusChem* **2017**, *10*, 1375-1379; g) M. Shetty, K. Murugappan,

T. Prasomsri, W. H. Green, Y. Román-Leshkov, *J. Catal.* **2015**, *331*, 86-97.

COMMUNICATION

Entry for the Table of Contents



Selective, active and stable heterogenous $\text{MoO}_x\text{-Pd/TiO}_2$ catalyst for hydrodeoxygenation of biomass derived feedstocks. High yields of 92% succinic acid production from tartaric acid are reported over multiple catalytic cycles. This results from in-situ reduction of supported MoO_x centers promoted by Pd on TiO_2 .